Risk-based seismic design of buildings using an efficient pushover analysis procedure

N. Lazar & M. Dolšek
University of Ljubljana, Slovenia

ABSTRACT: Present-generation procedures for earthquake-resistant design of buildings do not involve seismic risk assessment methodologies. Therefore the collapse risk of new buildings may not be acceptable for all stakeholders. This issue can be solved by adequate estimation of seismic risk in the design process of a building. By comparing the estimated risk with an acceptable risk it can eventually be decided whether or not the newly designed structure met all safety requirements. In this paper a procedure for risk-based design is summarized and demonstrated by means of an example of a 15-storey building. The procedure is iterative and involves envelope-based pushover analysis procedure, which was recently proposed and is capable of approximately simulating the effects of different system failure modes, whereas the collapse risk is assessed with consideration of appropriate integration limits. It is shown that the integration limits of the risk equation can affect final design.

1 INTRODUCTION

Current standards for earthquake-resistant design of buildings prescribe that buildings should be designed to withstand a design seismic action, which is defined for an earthquake recurrence interval associated with a limit state of interest, such as damage limitation or near-collapse limit state. Usually design procedures involve an elastic analysis method and de-sign acceleration spectrum, which implicitly takes into account the ability of inelastic energy absorption of the structural system. Thus, seismic risk of newly designed structures is only implicitly controlled through the *q*-factor (*R*-factor) concept and capacity design procedure. Therefore current standards for earthquake-resistant design of buildings do not control seismic risk to such an extent that would be acceptable for all types of structures and for all stakeholders. This issue can be solved by adequate estimation of seismic risk in the design process of a building, which would probably be the best approach for mitigation of earthquake losses in the future.

Several reliability-based frameworks for design of structures were proposed. Wen (2001) concluded that there are capabilities which allow development of risk-based, comprehensive, and yet practical design procedures familiar to engineers. Liu, Wen and Burns (2004) and Rojas, Pezeshk and Foley (2011) used genetic algorithms to determine an optimal structural configuration. Further, Fragiadakis and Papadrakakis (2008) proposed a fully automated design methodology for the optimum seismic design of reinforced concrete structures.

In the simplest approach, seismic risk can be described by means of the mean annual frequency of exceedance of a selected limit state, such as collapse of a building. This information incorporates effects of all possible earthquakes that could affect the structure at a given location. By comparing the estimated seismic risk with an acceptable or tolerated risk, as defined in the paper, it can eventually be decided whether the newly designed structure met all safety requirements or not.

In this paper a procedure for risk-based design (Lazar & Dolšek 2012) is summarized with an emphasis on the effect of integration limits on the collapse risk assessment of buildings and demonstrated by means of a 15-storey building. The risk-based design procedure is iterative and involves an envelope-based pushover analysis procedure (Brozovič & Dolšek 2013a), which enables consideration of different failure modes caused by ground motions, and risk assessment in terms of mean annual frequency of collapse based on a new closed-form formula, which takes into account appropriate integration limits as recently proposed by the authors of this paper. The integration limits are defined by assuming that the collapse can be exceeded only if the ground-motion intensity is greater than the minimum collapse intensity and that the ground-motion intensity cannot exceed the upper-bound ground-motion intensity, which can be estimated using results of the hazard analysis. Consideration of integration limits for collapse risk assessment provides less conservative estimates of probability of collapse as that obtained by assuming integration of the risk equation on the interval [0,∞) (Cornell 1996).

2 BRIEF OVERVIEW OF THE RISK-BASED DESIGN PROCEDURE

In general, the risk-based design procedure involves initial design, determination of the nonlinear structural model, definition of acceptable risk, an iterative risk assessment procedure based on envelope-based pushover analysis, guidelines for structural adjustments in order to achieve an optimal increase of ductility and strength in the current iteration, as well as probabilistic seismic hazard analysis, selection of ground motions, checks of final design based on nonlinear response history analysis performed for few ground motions and design of components, which are not simulated by the nonlinear model (Dolšek 2013). The flowchart of the first part of the design procedure is presented in Figure 1. For simplicity reasons only these steps of the risk-based design procedure were applied herein in order to design a 15-storey reinforced concrete building.

An initial structural configuration can be determined by using standards for earthquake-resistant design of buildings or by engineering judgment. For example, a simple initial structural configuration can be determined based on design of reinforcement for vertical loads with consideration of the maximum and minimum requirements for dimensions of structural elements and amount of reinforcement. In the following step seismic risk is estimated for the initial structural configuration and compared to the predefined acceptable risk, which is discussed later in the paper (Section 4.3). If the estimated risk exceeds the acceptable risk, the current structural configuration is adjusted in order to achieve reduction of seismic risk. Once the improved structural configuration is obtained, the seismic risk is re-evaluated. The described iterative procedure is repeated until the estimated seismic risk is lower than the acceptable risk. In the simplest case, the adjustments of the structure can be based on a trial and error procedure. However, it is foreseen that guidelines for efficient structural adjustment will be developed within the project supported by the Slovenian Research Agency (Dolšek 2013).

The main advantages of the proposed design procedure in comparison to that prescribed in Eurocode 8 are explicit simulation of structural damage due to earthquakes and explicit estimation of seismic risk. It should be noted that the proposed process does not involve definition of the design earthquake, but it requires detailed information regarding seismic hazard including deaggregation of seismic hazard.

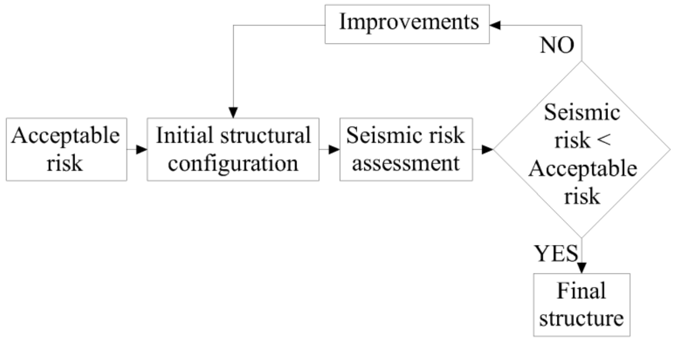

Figure 1. Flowchart of the proposed risk-based design procedure according to (Lazar & Dolšek 2012).

3 COLLAPSE RISK ASSESSMENT WITH CONSIDERATION OF APPROPRIATE INTEGRATION LIMITS

The assessment of collapse risk is often expressed in terms of the mean annual frequency (MAF) of collapse, which can be determined as follows (Cornell 1996, McGuire 2004)

$$\lambda_C = \int_0^\infty P\left(C \middle| IM = im\right) \cdot \left| \frac{\mathrm{d}H\left(im\right)}{\mathrm{d}im} \right| \cdot \mathrm{d}im \qquad (1)$$

where $P(C|IM = im)$ is the fragility or probability of collapse given the intensity measure im and $H(im)$ is the hazard, i.e. the mean annual frequency that the ground motion intensity exceeds im. If the hazard is assumed to be linear in log-log coordinates ($H = k_0 \cdot im^{-k}$) and if the fragility is expressed by means of the standard normal probability integral $\Phi[(\ln im - \ln im_{C,50})/\beta_C]$, then the approximate solution of Equation (1) can be achieved in closed-form (Cornell 1996, McGuire 2004):

$$P_C \approx H\left(im_{C,50}\right) \cdot e^{\frac{1}{2} \cdot k^2 \beta_C^2} \qquad (2)$$

where $im_{C,50}$ is the median value of the IM -based capacity (i.e. the median ground-motion intensity which causes collapse of the building), β_C is its logarithmic standard deviation and k is the slope of the hazard curve. Note that λ_C is replaced by P_C, which is the probability of collapse, since mean annual frequency of collapse is small (λ_C).

The MAF of collapse based on Equation (2) is a result of integrating the risk equation (Eq. (1)) in the range from 0 to ∞. However, this is not physically-consistent since all structures designed according to standards have a quite large collapse capacity. Therefore, a lower limit of collapse capacity (im_1) exists, since there is no ground motion which would cause collapse of a structure and have intensity lower than im_1. The upper integration limit im_2 also exists, since ground motions are constrained with several physical phenomena (Bommer et al. 2004). Due to these facts the MAF of collapse based on Equations (1) and (2) can become quite conservative. Authors of this paper recently derived the closed-form solution of Equation (1) if it is integrated in the interval [im_1, im_2]. If a lower-bound truncated lognormal distribution is assumed for the fragility function $P(C|IM = im)$, Equation (1) can be expressed as follows:

$$P_{C,im12} = P_C \cdot \left(\mathrm{erf}\left[\frac{1}{\sqrt{2}\beta_C} \left(k\beta_C{}^2 + \ln \frac{im_2}{im_{C,50}} \right) \right] - \right.$$
$$\left. - \mathrm{erf}\left[\frac{1}{\sqrt{2}\beta_C} \left(k\beta_C{}^2 + \ln \frac{im_1}{im_{C,50}} \right) \right] \right) \Big/ \left(1 + \mathrm{erf}\left[\frac{1}{\sqrt{2}\beta_C} \ln \frac{im_{C,50}}{im_1} \right] \right) \quad (3)$$

where erf[x] is the error function and is determined as follows:

$$\mathrm{erf}[x] = \frac{2}{\sqrt{\pi}} \int_0^x \exp\left[-\tau^2 \right] \mathrm{d}\tau \quad (4)$$

In the basic loop of the risk-based design procedure the fragility parameters $im_{C,50}$ and β_C are assessed by envelope-based pushover analysis (EPA) procedure (Brozovič & Dolšek 2013a). The EPA procedure utilizes several pushover analyses, which are performed for invariant horizontal force distributions corresponding to the first three vibration modes, and the inelastic response history analysis of a modal-based and so-called failure based SDOF models.

The failure-based SDOF models are based on the displacement vectors corresponding to the system failure modes of the 'second-mode' and 'third-mode' pushover curves. This is the only difference in definition of the failure-based SDOF models and the modal-based SDOF models. This makes the failure based SDOF models capable of predicting the global response of the structure with sufficient accuracy for the case when the 'first-mode' SDOF model provides inaccurate estimates. However, total demand is obtained by enveloping results associated with the three system failure modes. The approach for the determination of total demand is similar to that proposed by Socuoglu & Günay (2011). Therefore appropriate combination rules as in the case of the modal pushover analysis procedure (Chopra & Goel 2002) or correction factors introduced in the extended N2 method (Kreslin & Fajfar 2011) are not needed.

Note that Brozovič and Dolšek (2013b) have shown that collapse capacity based on the EPA procedure is assessed with useful degree of accuracy even in the case of taller buildings. More details regarding the EPA procedures are available elsewhere (Brozovič & Dolšek 2013a, 2013b).

3.1 *Lower limit of collapse capacity*

The value of the lower limit of collapse capacity depends on the structure and ground motions. In general it can be assessed by nonlinear response history analysis applied to the structural model of the entire building. This is not convenient since risk-based design is an iterative process. Therefore in this study the lower limit collapse capacity is obtained by EPA procedure, which is not computationally demanding.

In order to study when the incorporation of the lower limit collapse capacity for assessment of collapse risk becomes important, Equation (1) was integrated in the interval [im_1, ∞). The following result was obtained:

$$P_{C,im1} = P_C \cdot \frac{1}{2} \left(1 - \mathrm{erf}\left[\frac{1}{\sqrt{2}\beta_C} \left(k\beta_C^2 + \ln \frac{im_1}{im_{C,50}} \right) \right] \right) \quad (5)$$

The impact of the lower limit collapse capacity is estimated with the ratio between the probability of collapse obtained according to Equations (5) and (2) as presented in Figure 2. This ratio is presented as a function of β_C for different values of the hazard parameter k and ratios $im_1/im_{C,50}$. It is obvious that the impact of the lower limit collapse capacity increases with increasing parameters k, β_C and im_1. From Equation (5) the threshold value of im_1 was obtained:

$$im_{1,T} = im_{C,50} \cdot \exp\left[-2\beta_C - k\beta_C^2 \right] \quad (6)$$

The threshold value $im_{1,\mathrm{T}}$ can be compared to im_1, which is obtained for a set of ground motions. If im_1 is higher than $im_{1,T}$, then the impact of lower limit collapse intensity on the collapse risk may not be negligible.

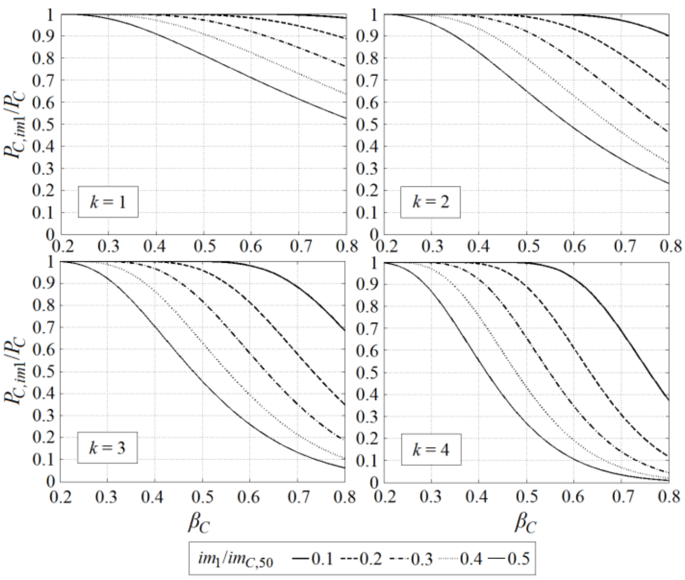

Figure 2. The ratio of $P_{C,im1}/P_C$ as a function of β_C presented for selected values of k and ratios $im_1/im_{C,50}$.

3.2 *Upper limit of ground-motion intensity*

Estimation of the upper integration limit of risk is in fact an issue of engineering seismology, which should be debated in the future. A need for prediction of the upper bound of a ground-motion parameter has been discussed among others by Strasser et al. (2004), but in a different context as that exposed herein. They have shown that the upper limit ground-motion intensity constantly increases with the extension of the period of ground motion recordings. Although a large number of strong ground motions is available today, it is probable that the strongest possible earthquakes have not yet been recorded, making the present estimates of maximum magnitudes and intensities inaccurate. Another issue is the level of truncation of intensity. For example, it has been previously shown for a region with moderate seismicity (Šket Motnikar & Lapajne 2004) that the intensities corresponding to a 10.000-year return period are not affected if the ground motion prediction model takes into account a truncation level equal or more than 3 standard deviations above the median value. However, the estimation of the upper limit ground motion should be consistent with the seismicity model and the ground-motion prediction model used in the hazard analysis.

In order to estimate the potential impact of the upper limit ground-motion intensity on the collapse risk, the risk equation (Eq. (1)) was integrated in the region [0, im_2]. The following result was obtained:

$$P_{C,im2} = P_C \cdot \frac{1}{2}\left(1 + \mathrm{erf}\left[\frac{1}{\sqrt{2}\beta_C}\left(k\beta_C^2 + \ln\frac{im_2}{im_{C,50}}\right)\right]\right) \quad (7)$$

Similarly as in the previous section, the impact of the upper bound ground-motion intensity is estimated with the ratio between the probability of collapse obtained according to Equations (7) and (2) (Fig. 3). In this case the opposite trend is observed in comparison to that discussed in the previous section. The impact of the upper limit ground-motion intensity reduces with increasing parameters k, β_C and im_2.

Similarly as for im_1 the threshold value of im_2 was obtained from Equation (7):

$$im_{2,T} = im_{LS,50} \cdot \exp\left[2\beta_{LS} - k\beta_{LS}^2\right] \quad (8)$$

Based on Equation (8) it can be concluded that the estimated upper bound ground-motion intensity for a region of interest has significant impact on the collapse risk if it is less than the threshold value $im_{2,T}$. In order to demonstrate the impact of im_2 on the design of the 15-storey building, the im_2 is assessed later in the paper (Section 4.4) with consideration of four ground motion prediction models and a truncation level of 2 and 2.5 standard deviations above the median.

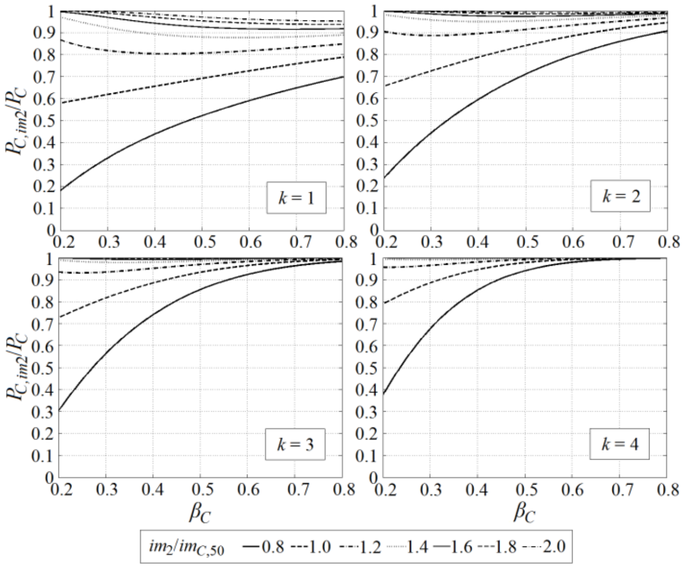

Figure 3. The ratio of $P_{C,im2}/P_C$ as a function of β_C presented for selected values of k and ratios $im_2/im_{C,50}$.

4 EXAMPLE

The proposed design procedure was used in order to design a 15-storey reinforced concrete building. It was assumed that the building is located in Ljubljana, Slovenia, i.e. in a moderate seismic region on soil type B. For illustration, the peak ground acceleration for a 475-year return period amounted to 0.30 g. Note that the initial structural configuration was based on Eurocode's provisions for minimum/maximum reinforcement ratio of the primary beams and columns corresponding to the ductility class medium. Additionally, the beams were rapidly designed for gravity loads only and the strong-column weak-beam concept was checked using the input results of the nonlinear structural model. For comparison reasons, the MAF of collapse was determined according to Equations (2) and (3), whereas the median peak ground acceleration at collapse $a_{g,C,50}$ and the corresponding standard deviation β_C was obtained by fitting a lognormal distribution to the sample of the $a_{g,C}$ (i.e. collapse capacity) determined based on the EPA procedure.

4.1 *Description of the initial structure and structural model*

The fifteen-storey frame building is a residential building (Fig. 4). The height of the first storey is 4 m, whereas the height of other storeys is 3 m. The slab thickness is 22 cm. Concrete C30/37 and reinforcing steel S500, class B, were adopted. All columns and beams of the initial structural configuration had the same dimensions and amount of reinforcement. The longitudinal reinforcement in all columns amounted to 1% of the cross-section area. Stirrups were based on the criteria of the minimum concrete confinement. The total mass of the building was 10643 t and the fundamental period amounted to 2.2 s.

A simplified nonlinear structural model was used, which fulfills requirements for the modeling of structures according to Eurocode 8. Inelastic rotational hinges were used in the beams and columns. For the beams, the plastic hinge was used for major axis bending only. For the columns, two independent plastic hinges for bending about the two principal axes were used. A linear negative post-capping stiffness is assumed after the maximum moment is achieved. These types of simplified nonlinear models were generated and analysed by using PBEE Toolbox (Dolšek 2010) in conjunction with OpenSees (2004). Note that the PBEE toolbox was recently extended in order to enable seismic performance assessment of frame buildings based on the EPA procedure (e.g. Brozovič and Dolšek 2013b).

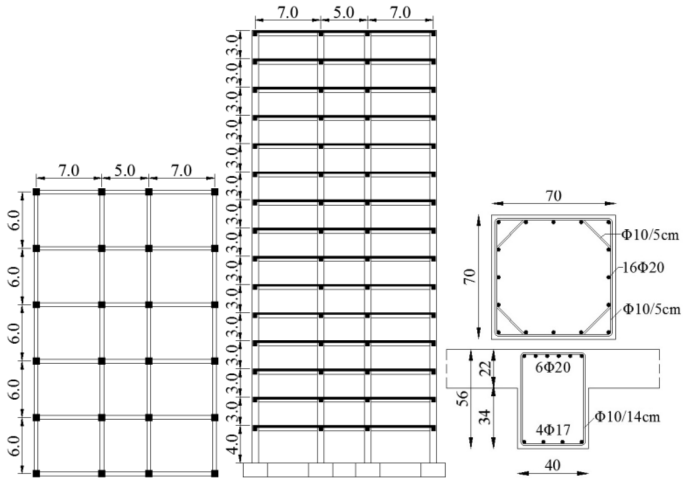

Figure 4. Plan, elevation view and reinforcement of beams and columns for the initial structural configuration of the fifteen-storey building.

4.2 *Seismic hazard and ground motion records*

The seismic hazard curve obtained by using EZ-FRISK (2012) (Baker 2011b) was used in the design. Note that EZ-FRISK contains a seismicity model for the central European region (Europe III), which is not consistent with the seismicity models used for determination of the seismic hazard maps for Slovenia (Lapajne et al. 2003). Based on the hazard curve, the hazard parameter $k = 2.9$ was obtained by fitting a straight line to the hazard curve in log-log coordinates with the method of least squares.

The ground-motion records were selected according to the procedure proposed by Jayaram et al. (2011). The uniform hazard spectrum prescribed by Eurocode 8 was used as a target response spectrum. It should be noted that hazard-consistent procedures (e.g. Baker 2011a, Bradley 2012) for the selection of ground motions were not applied in this study due to simplicity reasons and due to the lack of data (detailed hazard deaggregation is not available for the region of Slovenia). The ground motions were selected based on the magnitude between 5.5 and 7.5, fault distance between 5 and 50 km and shear wave velocity in the upper 30 m higher than 180 m/s.

The target uniform hazard spectrum, median response spectrum conditioned to the fundamental period of the analyzed structure and the corresponding 16th and 84th percentiles are presented in Figure 5. Note that it was herein assumed that the set of ground motions is also appropriate for the case when the peak ground acceleration is selected for an intensity measure, since the median spectrum conditioned to $T = 0$ is similar to that conditioned to the fundamental vibration period of the building.

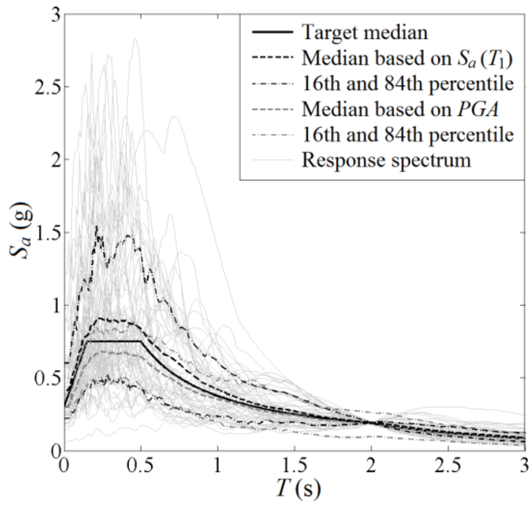

Figure 5. The target spectrum, spectra for each selected ground motion, the median spectrum of the selected ground motions and the corresponding 16th and 84th percentiles.

4.3 *Definition of acceptable risk*

In this study we distinguish between the acceptable and tolerated risk. Tolerated risk is associated with loss of human life, whereas the acceptable risk is associated with the remaining types of consequences, for example, with the collapse of the structure. The acceptable risk can be estimated by dividing the tolerated risk with the fatality rate, which is the conditional probability of loss of life given the collapse of the structure. For ductile reinforced concrete frames, which were investigated in this study, the fatality rate amounted to 0.15 (Jaiswal & Wald 2010).

For the purpose of this study the acceptable collapse risk was estimated on the basis of codes and guidelines (e.g. CEN 2004, ISO 1998, JCSS 2000) or from other models of acceptable/tolerated risk, such as the model proposed by Allen and that of CIRIA (e.g. Bhattacharya et al. 2001) or by Helm's model of tolerable risk (Helm 1996). More details are available elsewhere (e.g. Lazar & Dolšek 2012). However, herein it was assumed that the acceptable risk was based on Helm's model.

Helm (1996) divided risk into four regions; negligible, ALARP (as low as reasonably possible) region, possibly unjustifiable and unacceptable risk, as shown in Figure 6.

For the observed residential structure we assumed that 80 people will be exposed in the case of an event. The acceptable collapse risk was then obtained with consideration of the negligibility line (Fig. 6) and amounted to $8.3 \cdot 10^{-6}$ on an annual basis and $4.1 \cdot 10^{-4}$ for a period of 50 years.

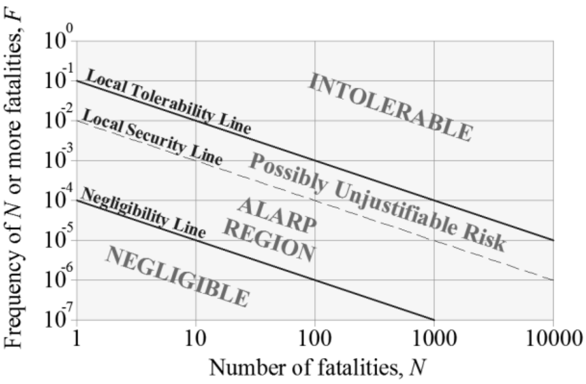

Figure 6. Helm's Frequency – Fatality curve according to (Helm 1996).

4.4 *Description of the design procedure*

The initial structural configuration was analyzed with the EPA procedure. The estimated collapse probability amounted to $3.6 \cdot 10^{-5}$ if based on Equation (2), which exceeded the acceptable collapse risk by a factor of 4.4. In order to assess the probability of collapse using Equation (3), the maximum intensity a_{g2} has to be estimated. Due to uncertainties presented in Section 3.2 it is suggested to use different ground-motion prediction (GMP) models for a given truncation level (e.g. 2 or 2.5 standard deviations σ above the median value) in order to assess a_{g2}. For the purpose of this study it was assumed that the worst-case scenario is an earthquake with magnitude 7, which is consistent with the seismic hazard analysis for Slovenia (Lapajne et al. 2003), and the source-to-site distance R_{jb} = 0 km. For comparison reasons two truncation levels (2σ and 2.5σ) were taken into account. Based on these assumptions, a_{g2} was calculated for the GMP models proposed by Sabetta and Pugliese (1996), Bindi et al. (2011), Akkar and Bommer (2010) and Peruš and Fajfar (2010) (Table 1).

Table 1. The upper peak ground accelerations corresponding to four GMP models taking into account 2 and 2.5 standard deviations above the median estimates.

GMP model	$a_{g2,2\sigma}$	$a_{g2,2.5\sigma}$
	g	g
Sabetta & Pugliese (1996)	2.15	2.63
Bindi et al. (2011)	2.14	3.16
Akkar & Bommer (2010)	1.43	1.97
Peruš & Fajfar (2010)	1.48	2.03

Based on Equation (8) it can be quickly estimated that the threshold value of the upper integration limit is 2.5 g, since k, $a_{g,C,50}$ and β_C of the initial structural configuration amounted, respectively, to 2.9, 2.24 g and 0.63. Therefore the collapse risk is affected by the upper integration limit when assessed by any of the four GMP models at a truncation level of 2σ and by the GMP models proposed by Akkar and Bommer or Peruš and Fajfar in the case of 2.5σ.

Similarly, we can evaluate if the lower intensity limit will have an impact on P_C by using Equation (6). For the initial structural configuration $a_{g1,T}$ was estimated to 0.20 g which is equal to $a_{g,1}$ based on the EPA procedure. Therefore the lower integration limit will not impact P_C.

Note that the $P_{C,im12}$ (Eq.(3)) of the initial structural configuration varied from 3.1 to $3.5 \cdot 10^{-5}$, which is from 5% to 15% less than the P_C calculated according to Equation (2). However, this reduction of collapse risk is quite negligible taking into account that the collapse risk of the initial design exceeded the acceptable collapse risk by a factor ranging from 3.7 to 4.2.

The initial structural configuration was therefore adjusted. Decision regarding the adjustments of the structural configurations was based on knowledge obtained from a previously performed sensitivity study on similar reinforced concrete frame buildings (Lazar & Dolšek 2012). Based on this study it was decided that for the 'second' structural configuration the amount of longitudinal reinforcement of the columns in the first eight storeys should be increased for 0.2% of the columns cross-section area. However, this adjustment was not sufficient. Several additional iterations were needed (Table 2) in order to achieve sufficient strength and ductility of the structure.

Table 2. Brief description of safety measures for the nine structural configurations. Note that the percentages refer to the area of cross-sections of columns or beams of the initial structural configuration.

Iteration	Adjustments in relation to previous iteration
1	Initial configuration
2	Added 0.2% column's reinforcement in storeys 1-8
3	Added 0.2% column's reinforcement in storeys 1-8
4	Added 5% beam's section size in storeys 1-5
5	Added 0.4% column's reinforcement in storeys 9-12
6	Added 10% column's section size in storey 1
7	Added 0.2% column's reinforcement in storeys 1-12
8	Added 10% column's section size in storey 1
9	Added 10% column's section size in storeys 1-3 and 0.2% column's reinforcement in storeys 1-3

Some characteristics of the nine structural configurations are presented in Table 3. It can be observed that the ratio between the total base shear and weight F_b/W increased from 5.1% to 6.7%. Similarly, the global ductility at the near collapse limit state (80% strength in post-capping range of the pushover curve) was also increased for about 20%.

For illustration, pushover curves and the relationship between the peak ground acceleration and the median value of the maximum storey drift ratio based on the EPA procedure are presented in Figures 7 and 8. It can be observed that the strength and deformation capacity were increased after each structural adjustment. However, the larger increment of strength, deformation capacity and $a_{g,C,50}$ was observed for the 'forth' structural configuration (see also Table 2).

Table 3. Some characteristics of the nine structural configurations.

Iteration	T_1	m	F_b/W	μ	$a_{g,C,50}$	β_C	a_{g1}
	s	t	%		g		g
1	2.20	10643	5.1	10.2	2.24	0.63	0.20
2	2.20	10647	5.2	10.7	2.33	0.62	0.21
3	2.20	10652	5.2	11.0	2.47	0.61	0.23
4	2.32	10696	6.4	10.2	2.75	0.58	0.28
5	2.32	10700	6.4	10.8	2.74	0.57	0.28
6	2.30	10711	6.4	11.1	2.72	0.56	0.29
7	2.30	10718	6.4	11.6	2.82	0.54	0.30
8	2.28	10730	6.5	11.8	2.79	0.53	0.31
9	2.25	10763	6.7	12.1	2.88	0.53	0.33

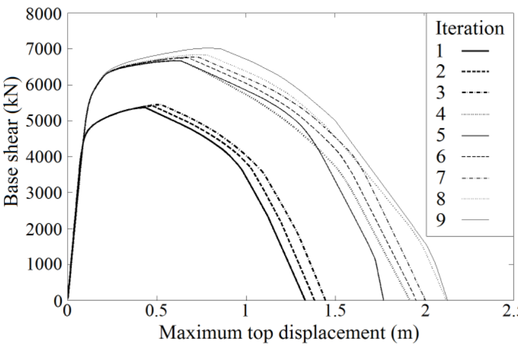

Figure 7. Pushover curves for all structural configurations of the 15-storey building.

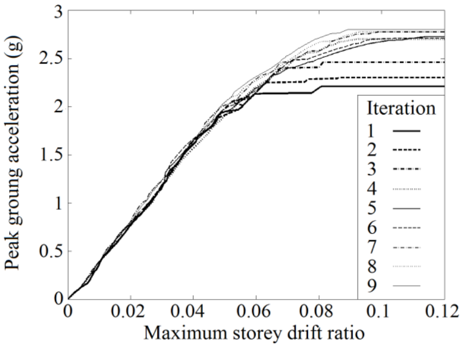

Figure 8. The relationship between the peak ground acceleration and the median value of the maximum storey drift ratio for all structural configurations of the 15-storey building.

For comparison reasons, the collapse risk based on Equations (2) and (3) is presented for all iterations within the design process taking into account the minimum and maximum value of the estimated upper integration limits, which correspond to truncation levels of 2σ and 2.5σ above the median. Results of this assessment are presented in Table 4.

Based on results presented in Table 4 it can be concluded that the collapse risk of the 'ninth' structural configuration is lower than the acceptable collapse risk according to Helm's model, even in the case if the effect of the upper integration limit on collapse risk was neglected. However, if the collapse risk was estimated by Equation (3) then it can be concluded that the final structure is overdesigned in most cases. Note that the effect of the upper integration limit on collapse risk did not affect the final design only for the case when a_{g2} was determined according to the GMP model proposed by Bindi et al. (2011) at a truncation level of 2.5σ above the median value (see bold numbers in Table 4). On the opposite side, the 'fifth' structural configuration was found sufficiently safe against collapse if the collapse risk was assessed by taking into account the upper integration limit determined with consideration of 2σ above the median peak ground acceleration according to the GMP model proposed by Akkar and Bommer (2010) (or Peruš and Fajfar (2010)). In this case the collapse risk of the final design was reduced by 42% of that based on Equation (2).

Note that the acceptable collapse risk was achieved by the seventh iteration for both other cases (i.e. max $a_{g,2,2\sigma}$ and min $a_{g,2,2.5\sigma}$),which still quite significantly affected the final design.

Table 4. Collapse risk according to Equations (2) and (3) for each structural configuration within the design process at different values of the upper intensity limit.

Iter.	$P_C \cdot 10^{-5}$	$P_{C,im12} \cdot 10^{-5}$			
		min $a_{g2,2\sigma}$	max $a_{g2,2\sigma}$	min $a_{g2,2.5\sigma}$	max $a_{g2,2.5\sigma}$
1	3.64	3.08	3.42	3.37	3.52
2	2.85	2.35	2.67	2.62	2.77
3	2.11	1.67	1.95	1.91	2.05
4	1.21	0.85	1.07	1.03	1.16
5	1.17	***0.81***	1.03	1.00	1.13
6	1.17	0.80	1.03	0.99	1.13
7	0.93	0.58	***0.80***	***0.76***	0.89
8	0.92	0.56	0.78	0.75	0.88
9	***0.80***	0.46	0.66	0.63	***0.76***

5 CONCLUSIONS

The iterative design procedure was used in order to design a 15-storey reinforced concrete frame building for collapse safety. The basic pushover-based method originally used to assess structural response was herein replaced by the EPA procedure, which enables approximate simulation of different system failure modes caused by earthquakes. Additionally, the collapse risk was estimated by taking into account appropriate lower and upper integration limits of the risk equation. Based on the presented example it was shown that such an approach enable less conservative risk assessment.

Although some components of the proposed design procedure are underdeveloped, the procedure has some advantages if compared to those prescribed in present-generation procedures for earthquake resistant design of structures. The main advantage of the proposed design procedure is an explicit estimation of seismic risk and better insight into the seismic response of different variants of the structure. Such information is meaningful and useful for decision-making regarding the optimal variant of the structure.

AKNOWLEDGEMENT

The results presented in this paper are based on work supported by the Slovenian Research Agency. This support is gratefully acknowledged.

REFERENCES

Akkar, S., Bommer, J.J, 2010. Empirical Equations for the Prediction of PGA, PGV, and SpectralAccelerations in Europe, the Mediterranean Region, and the Middle East. *Seismological Research Letters* 81(2): 195-206.

Baker J.W. 2011a. Conditional Mean Spectrum: Tool for ground motion selection. *Journal of Structural Engineering* 137(3): 322-331.

Baker, J.W. 2011b. Seismic hazard assessment for Ljubljana using EZ-FRISK. Personal communication, July 2011.

Bhattacharya, B., Basu, R., Ma, K., 2001. Developing target reliability for novel structures: the case of the Mobile Offshore Base. *Marine structures* 14: 37-58.

Bindi, D., Pacor, F., Luzi, L., Puglia, R., Massa, M.,Ameri, G., Paolucci, R. 2011. Ground motion prediction equations derived from the Italian strong motion database. *Bulletin of Earth-quake Engineering* 9(6): 1899-1920.

Bommer, J.J., Abrahamson, N.A., Strasser, F.O., Pecker, A., Bard, P.-Y., Bungum, H., Cotton, F., Fäh, D., Sabetta, F., Scherbaum, F., Studer, J. 2004. The challenge of defining upper bounds on earthquake ground motions. *Seismological Research Letters* 75(2): 82-95.

Bradley, B.A., 2012. A ground motion selection algorithm based on the generalized conditional intensity measure approach. *Soil Dynamics and Earthquake Engineering* 40: 48-61.

Brozovič, M., Dolšek, M. 2013a. Envelope-based pushover analysis procedure for seismic performance assessment of buildings. *Earthquake Engineering & Structural Dynamics* (in review).

Brozovič, M., Dolšek, M. 2013b. Envelope-based pushover analysis procedure for assessing the collapse risk of buildings. *11th International Conference on Structural Safety & Reliability; New York, NY, 16-20 June 2013.*

CEN, 2004. Eurocode 8: design of structures for earthquake resistance. Part 1: general rules, seismic actions and rules for buildings.

Chopra, A.K., Goel, R.K. 2002. A modal pushover analysis procedure for estimating seismic demands for buildings. *Earthquake Engineering and Structural Dynamics* 31(3): 561-582.

Cornell, C.A. 1996. Calculating building seismic performance reliability: a basis for multi-level design norms. *Eleventh World Conference on Earthquake Engineering, Mexico City, Mexico*, Paper No.2122.

Dolšek, M. 2010. Development of computing environment for the seismic performance assessment of reinforced concrete frames by using simplified nonlinear models. *Bulletin of Earthquake Engineering* 8(6). 1309-1329.

Dolšek, M. 2013. Concept of risk-based seismic design of buildings using methods of nonlinear analysis. In Papadrakakis, M., Papadopoulos, V., Plevris, V. (eds.), *4th ECCOMAS Thematic Conference on Computational Methods in Structural Dynamics and Earthquake Engineering; Kos Island, Greece, 12-14 June 2013.*

EZ-FRISK 2012. Software for Earthquake Ground Motion Estimation, version 7.62. Risk Engineering, Inc., Louisville, Colorado, USA.

Fragiadakis, M., Papadrakakis, M. 2008. Performance-based optimum seismic design of reinforced concrete structures. *Earthquake Engineering and Structural Dynamics* 37(6): 825-844.

Helm, P., 1996. Integrated Risk Management for Natural and Technological Disasters. *Tephra* 15(1): 5-19.

International Organization for Standardization (ISO), 1998. ISO 2394:1998(E) – General principles on reliability for structures.

Jaiswal, K.S., Wald, D.J. 2010. Development of a semi-empirical loss model within the USGS Prompt Assessment of Global Earthquakes for Response (PAGER) System. *9th US and 10th Canadian Conference on Earthquake Engineering: Reaching Beyond Borders*.

Jayaram, N., Lin, T., Baker, J.W. 2011. A Computationally Efficient Ground-Motion Selection Algorithm for Matching a Target Response Spectrum Mean and Variance. *Earthquake spectra* 27(3): 797-815.

Joint Committee on Structural Safety, 2000. Probabilistic model code – Part 1: Basis of Design.

Kreslin, M., Fajfar, P. 2011. The extended N2 method taking into account higher mode effects in elevation. *Earthquake Engineering and Structural Dynamics* 40(14): 1571-1589.

Lapajne, J., Šket Motnikar, B., Zupančič, P. 2003. Probabilistic Seismic Hazard Assessment Methodology for Distributed Seismicity. *Bulletin of the Seismological Society of America* 93(6): 2502-2515.

Lazar, N., Dolšek, M. 2012. Risk-based seismic design – An alternative to current standards for earthquake-resistant design of buildings. *15th World Conference on Earthquake Engineering, Lisbon, Portugal, September 24-28*.

Liu, M., Wen, Y.K., Burns, S.A. 2004. Life cycle cost oriented seismic design optimization of steel moment frame structures with risk-taking preference. *Engineering Structures* 26(10): 1207-1421.

McGuire, R.K. 2004. *Seismic hazard and risk analysis*. Oakland, California: Earthquake Engineering Research Institute.

Open System for Earthquake Engineering Simulation (OpenSEES) 2004. Pacific Earthquake Engineering Research Center (PEER), Univ. of California, Berkeley, CA. (http://opensees.berkeley.edu/)

Peruš, I., Fajfar, P. 2010. Ground-motion prediction by a non-parametric approach. *Earthquake engineering and structural dynamics* 39(12): 1395-1416.

Rojas, H.A., Foley, C., Pezeshk, S. 2011. Risk-Based Seismic Design for Optimal Structural and Nonstructural System Performance. *Earthquake Spectra* 27(3): 857-880.

Sabetta, F., Pugliese, A. 1996. Estimation of Response Spectra and Simulation of Nonstation-ary Earthquake Ground Motions. *Bulletin of Seismological Society of America* 86(2): 337-352.

Strasser, F.O., Bommer, J.J., Abrahamson, N.A. 2004. The need for upper bounds on seismic ground motion. *13th World Conference on Earthquake Engineering, Vancouver, Canada, August 2004.*

Sucuoglu, H., Günay, M.S. 2011. Generalized force vectors for multi-mode pushover analysis. *Earthquake Engineering and Structural Dynamics* 40(1): 55-74.

Šket Motnikar, B., Lapajne, J. 2004. Revised PSHA for NPP Krško – Annex A.1.2 The influence of truncation limit in attenuation models, PSR-NEK-2.7.2-Rev.1.

Wen, J.K. 2001. Reliability and performance-based design. *Structural Safety* 23(4): 407-428.